Journal of Assisted Reproduction and Genetics (2023) 40:65–73
https://doi.org/10.1007/s10815-022-02666-y

GENETICS

A novel heterozygous variant in *PANX1* causes primary infertility due to oocyte death

Juepu Zhou[1] · Meng Wang[1] · Juan Hu[1] · Zhou Li[1] · Lixia Zhu[1] · Lei Jin[1]

Received: 10 October 2022 / Accepted: 18 November 2022 / Published online: 5 December 2022

Abstract

Purpose Variants in the pannexin1 (*PANX1*) gene have been reported to be associated with oocyte death and recurrent in vitro fertilization failure. In this study, we performed genetic analysis in the patient with female infertility due to oocyte death to identify the disease-causing gene variant in the patient.

Methods We characterized one patient from a non-consanguineous family who had suffered from oocyte death and female infertility. Whole-exome sequencing and Sanger sequencing were used to identify the variant in the family. Western blot analysis was used to check the effect of the variant on PANX1 glycosylation pattern in vitro.

Results We identified a novel heterozygous *PANX1* variant (NM_015368.4 c.976_978del, (p.Asn326del)) associated with the phenotype of oocyte death in a non-consanguineous family, followed by an autosomal dominant (AD) mode. This variant showed a more delayed emergence of oocyte death than previously reported articles. Western blot analysis confirmed that the deletion variant of *PANX1* (c.976_978del) altered the glycosylation pattern in HeLa cells.

Conclusions Our findings expand the variant spectrum of *PANX1* genes associated with oocyte death and provide new support for the genetic diagnosis of female infertility.

Keywords *PANX1* · Variant · Oocyte death · Female infertility

Introduction

Reproductive diseases are a long-standing problem and have become more common in the world [1]. With the development of assisted reproductive technology (ART), including in vitro fertilization (IVF) and intracytoplasmic sperm injection (ICSI), millions of infertility couples have the chance to get a live birth [2]. However, the success rate of IVF/ICSI is still only around 30–40% [3]. Infertility and recurrent failure of IVF/ICSI attempts can occur in many processes, including gamete maturation, fertilization, zygote cleavage, and early embryonic development [1]. Recently, some research has revealed the genetic determinants of abnormalities in these processes. Several variant genes have been found to be responsible for the impediment of oocyte maturation (*PATL2*, *TUBB8*, *TRIP13*), zona pellucida abnormality (*ZP1*, *ZP2*, *ZP3*, *ZP4*), fertilization failure (*WEE2*, *TLE6*, *CDC20*), zygotic cleavage failure (*BTG4*), and early embryonic developmental arrest (*PADI6*, *NLRP2*, *NLRP5*, *REC114*, *KHDC3L*). These variants and genetic markers may lay the foundation for individualized genetic counseling and potential treatments for patients [3].

Zhou Li, Lixia Zhu, and Lei Jin contribute equally to the research.

✉ Zhou Li
lizhou618@hotmail.com

✉ Lixia Zhu
zhulixia027@163.com

✉ Lei Jin
leijintongjih@qq.com

Juepu Zhou
zhoujuepu@163.com

Meng Wang
tjmu_wm@163.com

Juan Hu
hujuan310@126.com

[1] Reproductive Medicine Center, Tongji Hospital, Tongji Medical College, Huazhong University of Science and Technology, No.1095, Jiefang Road, Wuhan 430030, China

Pannexin1 (PANX1) belongs to pannexins, a family of integral membrane proteins with distinct post-translational modifications, sub-cellular localization, and tissue distribution [4]. Cryo-electron microscopy shows that the PANX1 channel is assembled as a heptamer of seven identical subunits, each subunit consisted of a transmembrane domain with four membrane-spanning helices and folded extracellular and intracellular domains, and both the N and C termini resided on the cytoplasmic side [5–8]. PANX1 is a highly glycosylated membrane protein that exists as three species: the non-glycosylated protein (GLY0), the high mannose-type glycoprotein (GLY1), and the fully processed glycoprotein (GLY2) [9]. The GLY1 pattern is formed in the endoplasmic reticulum and then transported to the Golgi body to mature into GLY2 form, which is then targeted to the cell membrane [10]. PANX1 is a major ATP release and nucleotide permeation channel, playing important roles in a variety of physiological functions such as blood pressure regulation [11], apoptotic cell clearance [12], cancer progression and metastasis [13], and inflammatory response [14].

Recently, variants in *PANX1* have been found to cause "oocyte death" in ART, which means all the retrieved oocytes showed cytoplasmic shrinkage and darkening before or after fertilization [15–17]. Functional studies indicated that variants altered the PANX1 glycosylation pattern, thus resulting in aberrant PANX1 channel activity and ATP release [15]. These studies reveal that PANX1 plays a crucial role in oocyte development. Nonetheless, specific mechanisms and genetic factors of oocyte death are still unclear and need to be further explored.

In this study, we identified a heterozygous variant in *PANX1* in a non-consanguineous family with the phenotype of oocyte death after fertilization, followed by an autosomal dominant (AD) mode. This study showed a more delayed emergence of oocyte death than previously reported articles, which indicated the extent of the effect of variants on PANX1 function may be related to the difference in variant sites.

Methods

Human subjects and ethics approval

The infertility patient with the oocyte death phenotype was recruited from the Center of Reproductive Medicine, Tongji Hospital, Tongji Medical College, Huazhong University of Science and Technology. This study was approved by the ethics committee on human subject research at Huazhong University of Science and Technology (TJ-IRB20220450). Written informed consent was obtained from the participants.

Whole-exome sequencing (WES) and variant analysis

The details of the genetic analysis procedure have been well described previously [18, 19]. Genomic DNA was extracted from peripheral blood samples of the patient and her family members for WES to identify potential disease-causing variants according to the manufacturer's instructions. The exomes were captured and enriched using an Agilent SureSelect Human All Exon Kit, and next-generation sequencing (NGS) was performed on the Illumina HiSeq X-TEN platform. After quality control, the obtained raw FASTQ files were aligned to the human genome reference sequence (hg19/GRCh37) using Burrows-Wheeler Aligner (BWA) software. DNA sequence variants were detected using Genome Analysis Toolkit (GATK) software and then annotated with ANNOVAR software. Candidate variants identified in the participants were validated by Sanger sequencing analyses conducted on ABI PRISM 3500 Genetic Analyzer (Applied Biosystems, Foster City, CA).

The conservation of the amino acids in the variant site was analyzed among multiple species using MEGA software. The allele frequency of the variant in the general population was assessed using Genome Aggregation Database (GnomAD, http://gnomad.broadinstitute.org/). The pathogenicity of the variant was assessed using three online software: sorting intolerant from tolerant (SIFT, sift.jcvi.org), polymorphism phenotyping (PloyPhen2, genetics.bwh.harvard.edu/pph2), and mutation taster (http://www.mutaiontaster.org/). We used the structure model based on Cryo-EM structure of wild-type human pannexin1 channel (PDB ID, 6WBF/A) in the RCSB Protein Data Bank (https://www.rcsb.org/) and PyMOL software (https://pymol.org/2/) to analyze the effect of the variant in PANX1 protein.

Controlled ovarian stimulation, oocyte retrieval, and embryo culture

The patient underwent controlled ovarian stimulation, and gonadotropin dose is adjusted according to follicle size and hormone levels. When 2 or 3 dominant follicles reached a diameter of 18 mm, recombinant human chorionic gonadotropin (HCG, Merck Serono, Germany) was injected. Oocytes retrieval was performed 36–38 h after HCG administration guided by transvaginal ultrasound. Collected cumulus-oocyte complexes were then fertilized in conventional IVF. Fertilization check was performed 16–18 h after insemination, and the presence of two pronuclei was defined as normal fertilization. The fertilized zygotes were cultured in G1-plus medium (Vitrolife,

Sweden) to the cleavage stage until day 3. Embryo morphology was evaluated on day 2 and day 3 based on the number of blastomeres, rate of fragmentation, multinucleation of the blastomeres, and early compaction. The morphologies of oocytes, fertilization, and embryonic development were recorded by timelapse with images taken every 5 min. The morphology of gradual degeneration and death accompanied by cytoplasmic shrinkage and darkening is identified as oocyte death [15].

Plasmids construction

Wild-type (WT) human *PANX1* and mutated *PANX1* (p.Asn326del) were constructed and then recombined with the eukaryotic expression vector pcDNA3.1. A 3 × FLAG-tag was fused at the C-terminus of wild-type and mutated *PANX1*, respectively. The plasmids were constructed by OBiO Technology (Shanghai).

Cell culture and transfection

Human cervical cancer cell lines HeLa was gift from Cancer Biology Research Center of Tongji Hospital, Tongji Medical College, Huazhong University of Science and Technology. Cells were cultured in Dulbecco's Modified Eagle Medium/Nutrient Mixture F-12 (DMEM/F-12, KeyGEN Bio TECH, Jiangsu, China) supplemented with 1% penicillin/streptomycin (Servicebio, Wuhan, China) and 10% (v/v) fetal bovine serum (FBS, Wisten, Nanjing, China) and cultured at 37 ℃ in a humidified 5% CO_2 incubator. Cells were plated ~ 24 h before transfected and maintained until the cell density reached ~ 80% confluence. Before transfection, fresh medium with 4% FBS and without penicillin/streptomycin was added to each well. WT, mutated *PANX1* construct, and the pcDNA3.1 vector were transfected into Hela cells using liposomal transfection reagent (Yeasen, Shanghai, China) according to the manufacturer's instructions. Ten hours after transfection, fresh complete culture medium containing serum and antibiotics was replaced in each well, and cells were continued in culture.

Western blotting

Hela cells were harvested 36 h after transfection and washed three times with cold phosphate-buffered saline (PBS, Servicebio, Wuhan, China). Cells were lysed in RIPA lysis buffer with 2% of protease inhibitor (Servicebio, Wuhan, China). Supernatants were collected after centrifuged at 12,000 × *g* for 20 min at 4 ℃. Protein concentrations were determined with a BCA protein quantitative detection kit (Servicebio, Wuhan, China). Then, cell extracts were mixed with 5 × sodium dodecyl sulfate (SDS) loading buffer (Servicebio, Wuhan, China) and denatured by boiling for 10 min. Equal amounts of protein were separated using SDS–polyacrylamide gel electrophoresis and transferred to nitrocellulose filter membranes (Merck KGaA, Darmstadt, Germany). Non-specific binding sites were blocked for 1 h at room temperature with 5% non-fat milk diluted in Tris-buffered saline (Servicebio, Wuhan, China) containing 0.1% Tween-20 (TBST, Servicebio, Wuhan, China) and then incubated at 4 ℃ overnight with rabbit anti-PANX1 (1:1000 dilution, Cell Signaling Technology, kind gifts from Lei Wang's lab in Fudan University) or mouse anti-vinculin (1:1000 dilution, ABclonal, Wuhan, China) antibodies. The membranes were washed with TBST six times and incubated with goat anti-rabbit IgG secondary antibodies (1:2000 dilution, Servicebio, Wuhan, China) for 1 h at 37 ℃ followed by washing again with TBST six times. Finally, protein bands on the membranes were detected by ECL chemiluminescence kit (Vazyme, Nanjing, China) and imaged on a chemiluminescent imaging system (GeneGnome XRQ, Syngene, England). For densitometric analyses, protein bands on the blots were measured by ImageJ software.

Statistical analyses

All data are representative of three independent experiments. Values were analyzed by Student's *t*-tests when comparing experimental groups, and P values < 0.05 were considered statistically significant.

Results

Clinical characteristics of the proband

The proband was a 33-year-old woman with 10-year history of unexplained primary infertility. She had normal ovarian reserves and normal levels of sex hormones with basal follicle-stimulating hormone (FSH) 4.86 mIU/mL, luteinizing hormone (LH) 3.58 mIU/mL, and anti-Mullerian hormone (AMH) 10.15 ng/mL and a normal karyotype (46, XX). The seminal parameters of her husband showed 107.2 million per milliliter of sperm concentration, 56.5% progressive motility, and 5.2% normal sperm morphology per ejaculate. In the first IVF cycle in other hospital, she underwent a long gonadotropin-releasing hormone agonist (GnRH-a) protocol. The estradiol level on the day of hCG trigger was 1579.0 pg/ml. A total of 27 oocytes were retrieved, and all were successfully fertilized. However, except one viable embryo was cryopreserved on day 3, all the other fertilized oocytes degenerated and died within 60 h. The frozen-thawed embryo transfer was performed but failed to establish pregnancy. In the second IVF cycle in our hospital, she underwent a mild stimulation protocol. The estradiol level on the day of hCG trigger was

4744.8 pg/ml. A total of 19 oocytes were retrieved, 18 among them were MII stage. Subsequently, fifteen of the mature oocytes were successfully fertilized. Same as the first cycle, except one 8-cell embryo was cryopreserved on day 3, all the other fertilized oocytes degenerated and died within 60 h, and some of them died after finishing the first or second cleavage (Fig. 1). Furthermore, the frozen-thawed embryo transfer was performed but failed to establish pregnancy (Table 1).

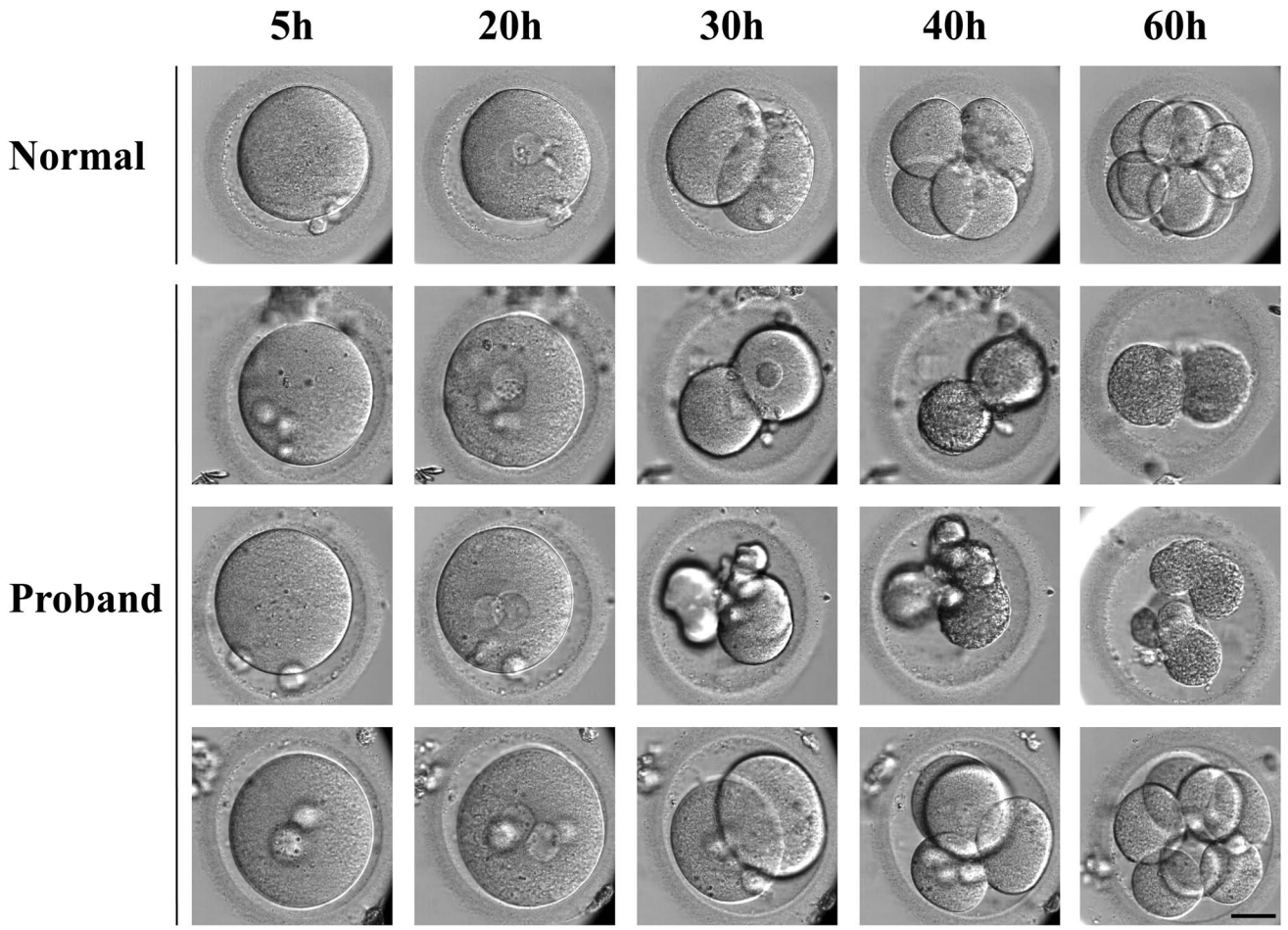

Fig. 1 Morphology of oocytes retrieved from control individuals and proband at 5 h, 20 h, 30 h, 40 h, and 60 h. Except one viable 8-cell embryo on day 3, all the other fertilized oocytes were degenerated and died within 60 h and some of them died after finishing the first or second cleavage. Scale bar, 40 μ

Table 1 Clinical characteristics of IVF attempts of the proband

Insemination method	Stimulation protocol	Total oocytes	MII oocytes	Fertilized oocytes	Oocytes that died or degenerated after fertilization	Outcomes
First IVF	Long GnRH-a	27	27	27	26	One frozen-thawed embryo was transferred but not pregnant
Second IVF	Mild stimulation	19	18	15	14	One frozen-thawed embryo (8-cell) was transferred but not pregnant

GnRH-a, gonadotropin-releasing hormone (GnRH) agonist; *IVF*, in vitro fertilization

Identification of heterozygous variants in PANX1

It has been reported that *PANX1* variants can cause female infertility characterized by oocyte death. Because of the oocyte death phenotype observed in the proband, WES was performed on the proband, and *PANX1* variant was mainly focused on. We found the heterozygous variant c.976_978del (p.Asn326del) of the *PANX1* gene (NM_015368.4), and no variants were identified in any other known disease-causing genes related to female infertility or other genes related to oocyte development. All members in the family underwent Sanger sequencing of the *PANX1* exons to further confirm the *PANX1* variant. As expected, the heterozygous *PANX1* variant carried by the proband was inherited from her father (Fig. 2A and B).

Function prediction of the PANX1 variant

As shown in Fig. 2C, variant c.976_978del is located in exon 4 and caused asparagine deletion at position 326 of PANX1 protein. The residue Asn326 was highly conserved across species (Fig. 2D). As shown in Table 2, the variant in the family is absent in the GnomAD. SIFT and PloyPhen2 were not applicable, and the deletion variant c.976_978del (p.Asn326del) of *PANX1* was predicted to be disease causing by mutation taster. We used the structure model 6WBF/A in the RCSB Protein Data Bank and PyMOL software to

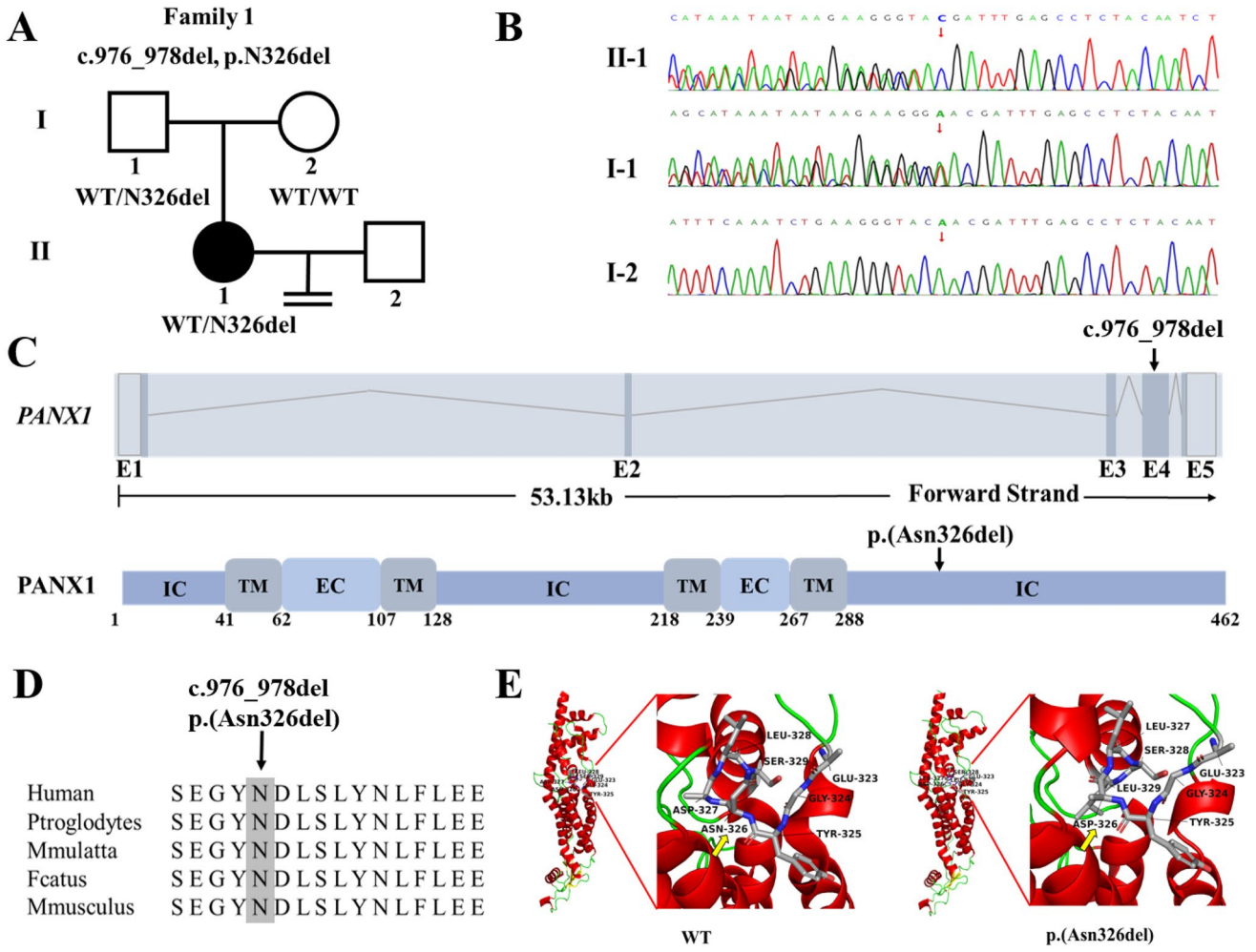

Fig. 2 Identification of variants in *PANX1*. **A** A pedigree with *PANX1* variant cause infertility with oocyte death phenotype. Squares indicate male family member, circles indicate female members, black solid circle indicates the proband, the equal sign indicates infertility, and "WT" indicates wild-type allele. **B** Sanger sequencing results of the proband and her family members. **C** Location of the newly identified heterozygous variant in *PANX1* exon and PANX1 protein. PANX1 protein. TM, transmembrane region; EC, extracellular region; IC, intracellular region. **D** Conservation analysis of the affected amino acid among eight species. **E** PyMOL-predicted structures of PANX1 variant are shown as cartoons. The structures of wild-type and mutated PANX1 proteins were modeled based on Cryo-EM structure of wild type human pannexin1 channel (PDB ID, 6WBF/A). Yellow arrows indicate the p.Asn326del variant; "WT" indicates wild-type allele

Table 2 Overview of the *PANX1* variant

Genomic position on Chr11	cDNA change	Protein change	Variant type	Inheritance	GnomAD	SIFT	PloyPhen2	Mutation taster
93,913,198_93,913,200	c.976_978del	p.Asn326del	Deletion	AD	Absent	NA	NA	Disease causing

AD, autosomal dominant; *NA*, not applicable

analyze the effect of the variant in PANX1. The variant (p.Asn326del, yellow arrow) leads to the link region of loop and alpha helix of mutated PANX1 protein being shorter than wild-type PANX1 (Fig. 2E).

Effect of heterozygous variant on PANX1 glycosylation *in vitro*

To evaluate the effect of the heterozygous variant on PANX1 glycosylation in vitro, WT and mutated *PANX1* construct were transfected into Hela cells for 36 h. Compared with WT PANX1, the p.Asn326del variant resulted in a significant reduction of GLY2 expression (Fig. 3A and B). These results indicated that the PANX1 variant (p.Asn326del) resulted in an altered glycosylation pattern in HeLa cells in vitro.

Discussion

In this study, we identified a heterozygous variant (c.976_978del (p. Asn326del)) in *PANX1* from a non-consanguineous family with the phenotype of oocyte death after fertilization. Compared to the previous reports, the variant showed a more mild phenotype with oocytes degenerated and died within 60 h, and some

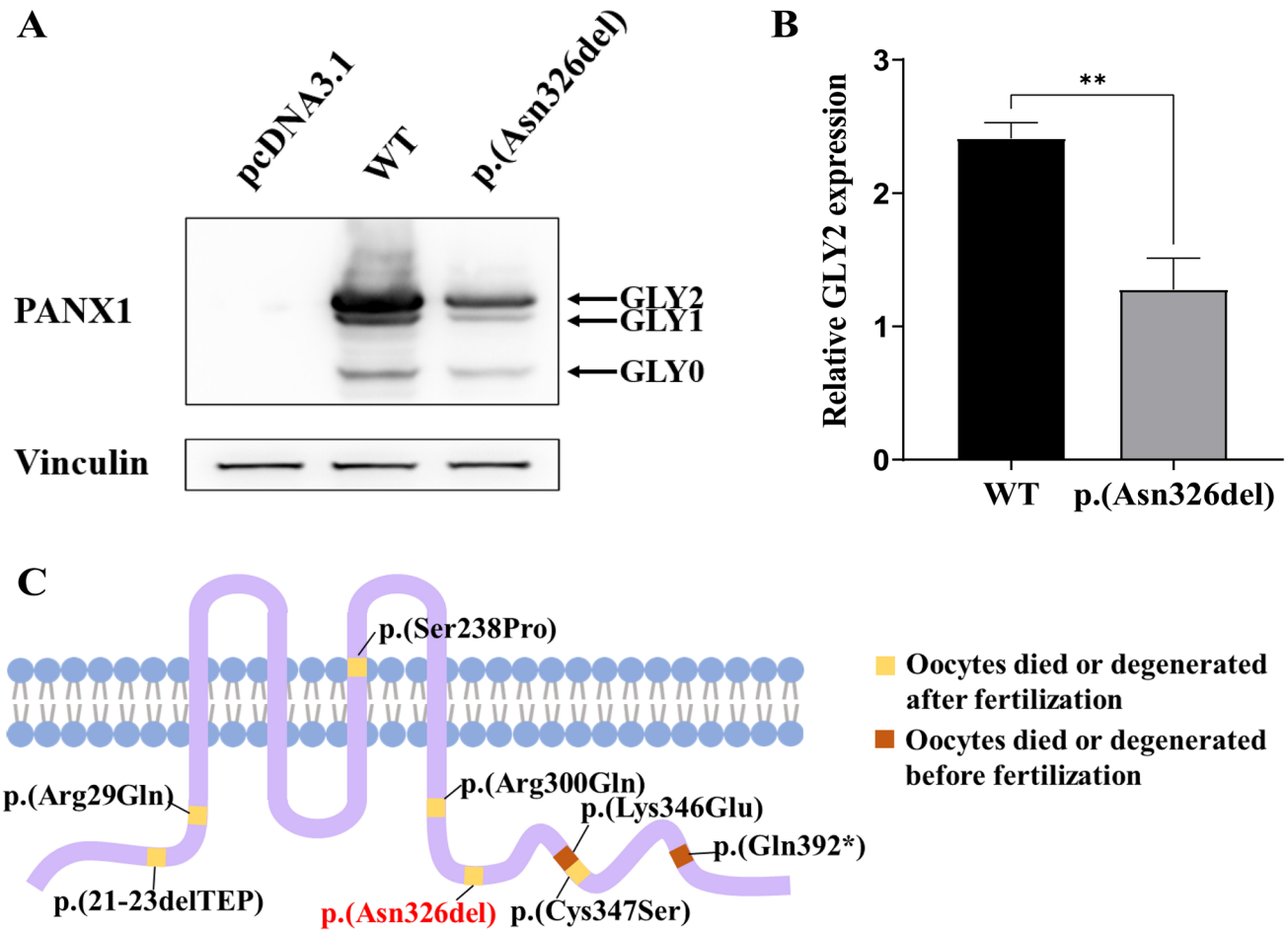

Fig. 3 Glycosylation assay of the *PANX1* variant. **A** Western blot analysis of HeLa cell extracts after transfection with WT or mutated PANX1 constructs. Vinculin was used as the loading control. WT, wild type. **B** The relative GLY2 expression of PANX1. The relative GLY2 expression of p.(Asn326del) variant was significantly reduced compared with WT. Three independent experiments were performed; $^{**}P < 0.01$. WT, wild type. **C** Currently reported PANX1 variants associated with oocyte death

of them died after finishing the first or second cleavage. And we confirmed that the heterozygous variant altered the PANX1 glycosylation pattern in cultured cells.

Because of its functional importance as a large-pore membrane channel by being permeable to ATP and many other metabolites [12, 20, 21], PANX1 has been found to be involved in many physiological and pathological processes and has become a hot topic of research [22, 23]. In 2019, Wang et al. firstly reported a new infertility phenotype called "oocyte death" and identified four heterozygous variants of *PANX1*, including c.C1174T (p.Gln392*), c.A1036G (p.Lys346Glu), c.G1040C (p.Cys347Ser), and c.61-69delACGGAG CCC (p.21_23delTEP) [15]. They found that variants altered glycosylation pattern and location of PANX1, and PANX1 channel showed aberrant activity and abnormal ATP release in oocytes [15]. This is the first time that PANX1 has been associated with female infertility. Subsequently, Sang et al. reported two homozygous variants of *PANX1* (c.T712C (p.Ser238Pro) and c.G899A (p.Arg300Gln)) caused oocytes with an autosomal recessive (AR) inheritance pattern [16]. Recently, Tan et.al reported the seventh identified variant of *PANX1* (c.G86A (p.Arg29Gln)) related to oocyte death [17]. In the present study, heterozygous variant c.976_978del (p. Asn326del) in *PANX1* was shown to cause oocyte death and followed by an AD inheritance pattern.

According to these reports, the severity of oocyte death is variable across variants. The p.Gln392* and p.Lys346Glu heterozygous variants of PANX1 caused oocytes died or degenerated before fertilization, while the other variants could retrieve normal viable oocytes and even viable embryos (p.Arg300Gln and our identified p.Asn326del). What is more, there are also differences in the inheritance patterns of different variants. The variants p.Ser238Pro and p.Arg300Gln resulted in oocyte death only in a homozygous state, while heterozygous p.Ser238Pro or p.Arg300Gln did not affect oocyte development. This may be related to the structural domain in which the variant site is located. Previous studies showed that the C-terminal domain and the N-terminal loop might serve as a channel gate for flux of ATP and other ions [21, 24, 25]. The C-terminal domain was found to block the main pore of PANX1 via a ball and chain mechanism. It acted as a pore plug that can be moved away or cleaved, resulting in opening of the channel [7, 21]. This may partly explain why variants p.Gln392* and p.Lys346Glu which are located at the C-terminal domain caused the more severe phenotype (Fig. 3C). In conclusion, these findings suggested that different locations of variants might appear different effects on the PANX1 protein and inheritance patterns might thereby be affected.

Because PANX1 is a glycoprotein that exists in different glycosylated forms [26], and the level of glycosylation is critical for the cellular localization and the function of the channel [27], glycosylation assay is an important part of assessing PANX1 function. Previous research showed that variants of *PANX1* altered the PANX1 glycosylation pattern, and we therefore transfected WT and mutated *PANX1* constructs in Hela cells to detect the expression of PANX1 in vitro. As shown in our results, PANX1 with variant p.Asn326del still had the GLY2 species, but at a significantly lower level compared to WT (Fig. 3A and B). It may explain why our patient showed more delayed onset of oocyte death and some of them died after finishing the first or second cleavage (Fig. 1). This may further suggest that the degree of phenotype severity is dependent on the impairment of PANX1 glycosylation resulting from the different variants.

Although the effects of genetic determinants of abnormalities on oocyte and embryo development can be severe, variants in some related genes can still result in successful pregnancies, such as *PADI6* [28], *ZP1* [29, 30], and *ZP2* [30]. However, none of the infertility patients with *PANX1* variants reported so far has achieved successful pregnancy by ART [15–17]. Notably, Tan et al. reported that the variant c. 86G > A of *PANX1* exhibited reduced penetrance. The aunt of the proband, who was also the heterozygous missense variant carrier, had given birth to a son 17 years ago by herself without ART treatment or oocyte donation program [17]. In addition, good quality embryos were also produced from our patient with variant c.976_978del of *PANX1* during IVF treatment (Fig. 1). Therefore, whether patients with *PANX1* variants could get pregnancy opportunities with ART remains doubtful and needs a long-time follow up.

Although preliminary studies on *PANX1* variants causing oocyte death have been conducted, there are still some questions that need further research. For instance, the exact molecular mechanism of how fertilization accelerated the death of oocytes is still unclear. This may be related to the series of changes that the oocyte undergoes after fertilization, including Ca^{2+} oscillations [31], cortical granule exocytosis [32], the resumption of the second phase of meiosis [33], and extrusion of the second polar body [34]. Therefore, variant-induced alterations in PANX1 function and oocyte death still need further exploration.

Conclusion

In conclusion, we have identified the heterozygous variant c.976_978del (p.Asn326del) in *PANX1* as responsible for oocyte death and female infertility. Our finding expands the variant spectrum of *PANX1* and provides additional genetic markers for infertility patients.

Acknowledgements We would like to thank Qing Sang and Lei Wang from Fudan University for providing the gift of PANX1 antibody. We also thank the patient and her family for their participation and support in this study.

Author contribution Juepu Zhou: Literature review, writing and revising of text and tables. Meng Wang: Lead for prediction model, literature review, writing and revising. Juan Hu: Tables, figures, literature review. Zhou Li: Literature review and revising. Lixia Zhu: Conception and design, writing and revising. Lei Jin: Primary supervisor, conception and design, writing and revising.

Funding This work was supported by the research grants from the National Key Research & Development Program of China (2021YFC2700603) and Health Commission of Hubei Province scientific research project (WJ2021M110).

Data Availability All data generated and analyzed in this study are included in this published manuscript.

Declarations

Ethics approval and consent to participate This study has been approved by the Ethics Committee of Tongji Hospital of Tongji Medical College of Huazhong University of Science and Technology. Reference number for ethics approval is TJ-IRB20220450. Written informed consent was obtained from the participants.

Conflict of interest The authors declare no competing interests.

References

1. Fei C-F, Zhou L-Q. Gene mutations impede oocyte maturation, fertilization, and early embryonic development. BioEssays. 2022;44(10):e2200007.
2. DeAngelis AM, Martini AE, Owen CM. Assisted reproductive technology and epigenetics. Semin Reprod Med. 2018;36(3–04):221–32.
3. Sang Q, Zhou Z, Mu J, Wang L. Genetic factors as potential molecular markers of human oocyte and embryo quality. J Assist Reprod Genet. 2021;38(5).
4. Whyte-Fagundes P, Zoidl G. Mechanisms of pannexin1 channel gating and regulation. Biochim Biophys Acta Biomembr. 2018;1860(1):65–71.
5. Jin Q, Zhang B, Zheng X, Li N, Xu L, Xie Y, et al. Cryo-EM structures of human pannexin 1 channel. Cell Res. 2020;30(5):449–51.
6. Qu R, Dong L, Zhang J, Yu X, Wang L, Zhu S. Cryo-EM structure of human heptameric Pannexin 1 channel. Cell Res. 2020;30(5):446–8.
7. Deng Z, He Z, Maksaev G, Bitter RM, Rau M, Fitzpatrick JAJ, et al. Cryo-EM structures of the ATP release channel pannexin 1. Nat Struct Mol Biol. 2020;27(4):373–81.
8. Michalski K, Syrjanen JL, Henze E, Kumpf J, Furukawa H, Kawate T. The Cryo-EM structure of pannexin 1 reveals unique motifs for ion selection and inhibition. Elife. 2020;9.
9. Penuela S, Bhalla R, Gong X-Q, Cowan KN, Celetti SJ, Cowan BJ, et al. Pannexin 1 and pannexin 3 are glycoproteins that exhibit many distinct characteristics from the connexin family of gap junction proteins. J Cell Sci. 2007;120(Pt 21):3772–83.
10. Boassa D, Ambrosi C, Qiu F, Dahl G, Gaietta G, Sosinsky G. Pannexin1 channels contain a glycosylation site that targets the hexamer to the plasma membrane. J Biol Chem. 2007;282(43):31733–43.
11. Billaud M, Chiu Y-H, Lohman AW, Parpaite T, Butcher JT, Mutchler SM, et al. A molecular signature in the pannexin1 intracellular loop confers channel activation by the α1 adrenoreceptor in smooth muscle cells. Sci Signal. 2015;8(364):ra17.
12. Chekeni FB, Elliott MR, Sandilos JK, Walk SF, Kinchen JM, Lazarowski ER, et al. Pannexin 1 channels mediate "find-me" signal release and membrane permeability during apoptosis. Nature. 2010;467(7317):863–7.
13. Di Virgilio F, Sarti AC, Falzoni S, De Marchi E, Adinolfi E. Extracellular ATP and P2 purinergic signalling in the tumour microenvironment. Nat Rev Cancer. 2018;18(10):601–18.
14. Idzko M, Ferrari D, Eltzschig HK. Nucleotide signalling during inflammation. Nature. 2014;509(7500):310–7.
15. Sang Q, Zhang Z, Shi J, Sun X, Li B, Yan Z, et al. A pannexin 1 channelopathy causes human oocyte death. Sci Transl Med. 2019;11(485).
16. Wang W, Qu R, Dou Q, Wu F, Wang W, Chen B, et al. Homozygous variants in PANX1 cause human oocyte death and female infertility. Eur J Hum Genet. 2021;29(9):1396–404.
17. Wu X-W, Liu P-P, Zou Y, Xu D-F, Zhang Z-Q, Cao L-Y, et al. A novel heterozygous variant in PANX1 is associated with oocyte death and female infertility. J Assist Reprod Genet. 2022;39(8):1901–8.
18. Zhou X, Zhu L, Hou M, Wu Y, Li Z, Wang J, et al. Novel compound heterozygous mutations in WEE2 causes female infertility and fertilization failure. J Assist Reprod Genet. 2019;36(9):1957–62.
19. Liu Z, Xi Q, Zhu L, Yang X, Jin L, Wang J, et al. TUBB8 mutations cause female infertility with large polar body oocyte and fertilization failure. Reprod Sci. 2021;28(10):2942–50.
20. Nielsen BS, Toft-Bertelsen TL, Lolansen SD, Anderson CL, Nielsen MS, Thompson RJ, et al. Pannexin 1 activation and inhibition is permeant-selective. J Physiol. 2020;598(2):361–79.
21. Narahari AK, Kreutzberger AJ, Gaete PS, Chiu Y-H, Leonhardt SA, Medina CB, et al. ATP and large signaling metabolites flux through caspase-activated pannexin 1 channels. Elife. 2021;10.
22. Yang K, Xiao Z, He X, Weng R, Zhao X, Sun T. Mechanisms of pannexin 1 (PANX1) channel mechanosensitivity and its pathological roles. Int J Mol Sci. 2022;23(3).
23. Laird DW, Penuela S. Pannexin biology and emerging linkages to cancer. Trends Cancer. 2021;7(12):1119–31.
24. Kuzuya M, Hirano H, Hayashida K, Watanabe M, Kobayashi K, Terada T, et al. Structures of human pannexin-1 in nanodiscs reveal gating mediated by dynamic movement of the N terminus and phospholipids. Sci Signal. 2022;15(720):eabg6941.
25. Mou L, Ke M, Song M, Shan Y, Xiao Q, Liu Q, et al. Structural basis for gating mechanism of Pannexin 1 channel. Cell Res. 2020;30(5):452–4.

26. Bhat EA, Sajjad N. Human pannexin 1 channel: insight in structure-function mechanism and its potential physiological roles. Mol Cell Biochem. 2021;476(3):1529–40.
27. Penuela S, Simek J, Thompson RJ. Regulation of pannexin channels by post-translational modifications. FEBS Lett. 2014;588(8):1411–5.
28. Qian J, Nguyen NMP, Rezaei M, Huang B, Tao Y, Zhang X, et al. Biallelic PADI6 variants linking infertility, miscarriages, and hydatidiform moles. Eur J Hum Genet. 2018;26(7):1007–13.
29. Cao Q, Zhao C, Zhang X, Zhang H, Lu Q, Wang C, et al. Heterozygous mutations in ZP1 and ZP3 cause formation disorder of ZP and female infertility in human. J Cell Mol Med. 2020;24(15):8557–66.
30. Chu K, He Y, Wang L, Ji Y, Hao M, Pang W, et al. Novel ZP1 pathogenic variants identified in an infertile patient and a successful live birth following ICSI treatment. Clin Genet. 2020;97(5):787–8.
31. Wang F, Yuan R-Y, Li L, Meng T-G, Fan L-H, Jing Y, et al. Mitochondrial regulation of [Ca]i oscillations during cell cycle resumption of the second meiosis of oocyte. Cell Cycle. 2018;17(12):1471–86.
32. Rojas J, Hinostroza F, Vergara S, Pinto-Borguero I, Aguilera F, Fuentes R, et al. Knockin' on egg's door: maternal control of egg activation that influences cortical granule exocytosis in animal species. Front Cell Dev Biol. 2021;9:704867.
33. Pan B, Li J. The art of oocyte meiotic arrest regulation. Reprod Biol Endocrinol. 2019;17(1):8.
34. Georgadaki K, Khoury N, Spandidos DA, Zoumpourlis V. The molecular basis of fertilization (Review). Int J Mol Med. 2016;38(4):979–86.